

# High Sensitivity of In Vivo Detection of Gold Nanorods Using a Laser Optoacoustic Imaging System

Mohammad Eghtedari,<sup>†</sup> Alexander Oraevsky,<sup>‡</sup> John A. Copland,<sup>§</sup>  
Nicholas A. Kotov,<sup>||</sup> Andre Conjusteau,<sup>‡</sup> and Massoud Motamedi<sup>\*†</sup>

*Center for Biomedical Engineering, University of Texas Medical Branch, Galveston, Texas 77555, Fairway Medical Technologies, Houston, Texas 77099, Department of Cancer Biology, Mayo Clinic Cancer Center, Mayo Clinic College of Medicine, Jacksonville, Florida 32224, and Department of Chemical Engineering, University of Michigan, Ann Arbor, Michigan 48109*

Received March 8, 2007; Revised Manuscript Received June 1, 2007

## ABSTRACT

The development of a contrast agent for a laser optoacoustic imaging system (LOIS) can significantly widen preclinical and clinical applications of this imaging modality for early detection of cancerous tumors. Gold nanorods were engineered to enhance the contrast for optoacoustic imaging. Under in vivo conditions, 25  $\mu\text{L}$  of gold nanorods solution at a concentration of 1.25  $\mu\text{M}$  were injected into nude mice and detected using a single-channel acoustic transducer. LOIS was used to visualize the distribution of gold nanoparticles at a concentration of 125  $\mu\text{M}$  in vivo when 100  $\mu\text{L}$  of solution of gold nanoparticles was delivered subcutaneously. Our results suggest that LOIS can be used for in vivo detection of gold nanorods at low concentrations and the nanoparticles can be engineered to enhance the diagnostic power of optoacoustic imaging.

Molecular targeting of nanoparticles to cancer cells and the tracking of these targeted particles in vivo is suggested for the detection of tumors in their early stages.<sup>1,2</sup> Currently, fluorescent and superparamagnetic nanoparticles are under clinical investigation to aid in the diagnosis of cancer; however, light scattering within tissue limits the spatial resolution of conventional optical methods in locating fluorescent nanoparticles deep within tissue.<sup>1,3</sup> The tracking of superparamagnetic nanoparticles requires very sophisticated, complex, and expensive devices. Thus, the development of a new imaging technique that enables the tracking of targeted nanoparticles in vivo could significantly expand the applications of nanotechnology in modern medicine.

Laser optoacoustic imaging system is a novel modality that combines the spectral selectivity of molecular excitation by laser light with the high resolution of ultrasound detection, thereby overcoming the limitations of pure optical and ultrasound-based methods.<sup>4</sup> In optoacoustic imaging, tissue is irradiated with a short laser pulse that can be selected at

the near-infrared (NIR) region of the spectrum to enhance light penetration and probing of tissue.<sup>5</sup> Within most tissue, light-absorbing components such as hemoglobin of blood absorb photons, transfer energy in the form of heat to surrounding tissue, which then undergoes thermoelastic expansion, resulting in generation of acoustic waves that can be detected on the surface of the tissue using acoustic transducers operating in a wide ultrasonic frequency band. By using an array of acoustic transducers and applying filtered back projection algorithms to the time-resolved optoacoustic signals, LOIS renders an image.<sup>4,6</sup> Like the contrast of conventional optical methods, optoacoustic contrast is dependent on the difference in the optical absorption of objects to render an image, but unlike conventional optical methods, it uses ultrasound waves to locate objects. Because ultrasound waves can travel through tissue with minimal scattering and attenuation, LOIS is capable of locating optically absorbing objects deep within tissue. Thus, the main advantage of LOIS over conventional optical methods is its ability to detect objects deep within biological tissue. The optoacoustic method is also superior to pure ultrasound because it uses optical absorption as a source of contrast, which leads to far greater contrast between diseased and healthy tissue than that based upon acoustic impedance.

Gold nanoparticles possess a tunable and exceptionally strong optical absorption due to their plasmon resonance.<sup>7,8</sup>

\* Corresponding author. E-mail: mmotamed@utmb.edu. Telephone: (409)772-6118. Fax: (409)772-0751. Address: Center for Biomedical Engineering, University of Texas Medical Branch, 301 University Boulevard, UTMB Route 0456, Galveston, TX 77555-0456.

<sup>†</sup> Center for Biomedical Engineering, University of Texas Medical Branch.

<sup>‡</sup> Fairway Medical Technologies.

<sup>§</sup> Department of Cancer Biology, Mayo Clinic Cancer Center, Mayo Clinic College of Medicine.

<sup>||</sup> Department of Chemical Engineering, University of Michigan.

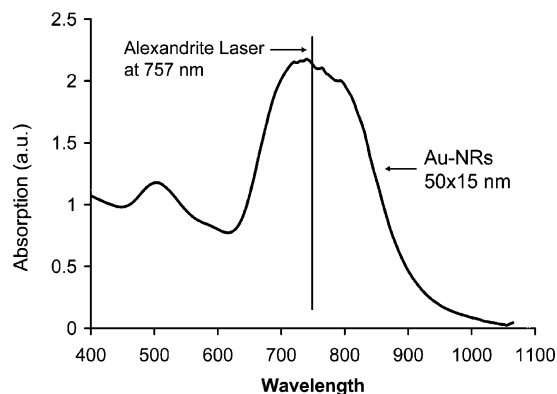


**Figure 1.** Absorption spectrum of raw Au-NRs with an approximate size of 50 nm × 15 nm. The peak absorption is close to the emission wavelength of the alexandrite laser at 757 nm.

Strong optical absorption results in the generation of detectable acoustic waves upon pulse laser irradiation. In the past, we have demonstrated the use of spherical gold nanoparticles for the molecular-specific detection of cancer cells *in vitro* using optoacoustic methods.<sup>9</sup> Considering the peak absorption of spherical gold nanoparticles that are located at the visible region of the spectrum and the fact that visible light cannot penetrate deep within tissue, one would conclude that spherical gold nanoparticles are not suitable for *in vivo* optoacoustic detection. Unlike visible light, NIR light penetrates deep within tissue.<sup>10</sup> Spherical gold nanoshells absorbing in the NIR have been applied as an optoacoustic contrast agent *in vivo*, however, without specific targeting to cellular receptors.<sup>11</sup> Previously, we proposed to employ gold nanorods as a contrast agent for optoacoustic imaging<sup>12</sup> due to their advantages relative to gold nanospheres and nanoshells: (a) resonance optical absorption of gold nanorods is substantially stronger than that of nanoshells<sup>13</sup> and (b) nanorods can be made much smaller than nanoshells, which increases their efficiency in targeting specific cellular receptors.<sup>14</sup> These properties of gold nanorods attracted attention of research groups developing pure optical methods.<sup>15</sup>

In this work, gold nanorods (Au-NRs) with an average size of 50 nm × 15 nm were fabricated using a seed-mediated method.<sup>16</sup> This method allows the creation of gold nanorods with desirable dimensions and to tune their plasmon resonance wavelength to 760 nm. This wavelength was selected because the light absorption of tissue is minimal, while hemoglobin has a local absorption peak, and thus deep irradiation of tissue is possible by using a commercially available alexandrite laser at 757 nm. The absorption spectrum of Au-NRs was measured using a Cary 50 spectrophotometer. An “as synthesized” solution of Au-NRs was estimated to contain  $7.5 \times 10^9$  NRs per mL.<sup>16</sup> Figure 1 shows the absorption spectrum of fabricated Au-NRs and the emission wavelength of the alexandrite laser at 757 nm.

Raw Au-NRs were suspended in a solution that was saturated with cetyl trimethyl ammonium bromide (CTAB), which is a toxic surfactant.<sup>17</sup> The removal of CTAB from solution causes particle aggregation, which means that raw Au-NRs cannot be used *in vivo*. To address this issue, Au-NRs were stabilized by covalent attachment of poly(ethylene

glycol), which allows the removal of free CTAB from the nanoparticle solution without causing aggregation.<sup>18</sup> Au-NRs (10 mL) was incubated overnight with 1 mL of 2 mM potassium carbonate and 0.1 mL of 1 mM methoxy-polyethylene glycol thiol (mPEG-thiol) with a molecular weight of 5000 Da (Nektar, Huntsville, AL) at room temperature. Extra mPEG-thiol was removed from solution by two rounds of centrifugation, and then Au-NRs were resuspended in phosphate buffered saline (PBS). Unlike raw Au-NRs, PEGylated Au-NRs were stable when suspended in PBS in the absence of free CTAB. Optical spectroscopy showed that the shift of the peak absorption wavelength of Au-NRs after PEGylation was negligible (data not shown). Alternatively, Au-NRs were coated with poly(sodium-4-styrenesulfonate) (PSS, Sigma) as described in the literature.<sup>19</sup> Like PEGylated particles, PSS-coated Au-NRs could be used *in vivo*.

The first optoacoustic experiment was aimed at the detection of Au-NRs at low concentrations through a thick scattering media. To do this, a disk-shaped phantom was made of a 10% gelatin and 1% whole milk solution to simulate the scattering properties of the tissue. The thickness of the phantom was approximately 4 cm. The phantom was placed on top of a single-channel acoustic transducer that was made of a 10 mm × 10 mm square shape polyvinylidene difluoride (PVDF) piezoelectric film with 110 μm thickness. The transducer was then mounted on acoustic impedance matching material with strong ultrasound absorption property. The transducer was interfaced with a Tektronix oscilloscope (TDS 3012B, Richardson, TX) through a low-noise wide-band amplifier with high input impedance and a gain of 60 dB (LAT-06AB-0700, Fairway Medical Technologies, Houston, TX). The transducer sensitivity was  $\sim 30 \mu\text{V}/\text{Pa}$  within the ultrasonic frequency band from 50 kHz to 5 MHz. Ultrasound gel was applied to ensure impedance matching between the transducer and the phantom. An alexandrite laser operating at 757 nm with a pulse duration of 75 ns was used to illuminate the sample with a relatively homogeneous beam distribution, delivering an average fluence of 6 mJ/cm<sup>2</sup>. For each measurement, the optoacoustic signal was averaged over 16 laser pulses. The optoacoustic signal was recorded when 100 μL of water (control), Au-NRs at a concentration of  $7.5 \times 10^8$  NRs per mL (1.25 pM), and Au-NRs at a concentration of  $7.5 \times 10^9$  NRs per mL (12.5 pM) was applied dropwise on the top surface of the phantom using a pipet. Recorded optoacoustic signals are shown in Figure 2.

In Figure 2, the y-axis is the amplitude of the recorded signal in volts and the x-axis is the time of arrival of the signal to the transducer following pulsed laser irradiation. The distance between the target and transducer can be calculated by multiplying the time of arrival by the speed of sound in the phantom ( $\sim 1.5 \text{ mm}/\mu\text{s}$ ); in our case,  $\sim 37 \text{ mm}$ . This experiment shows that: (1) Au-NRs are detectable *in vitro* using an optoacoustic method at a concentration of  $7.5 \times 10^8$  NPs/mL (1.25 pM) and (2) the amplitude of optoacoustic signal is proportional to the concentration of Au-NRs.

Detection of nanoparticles through a biological tissue is important because the ultimate goal of our project is to detect

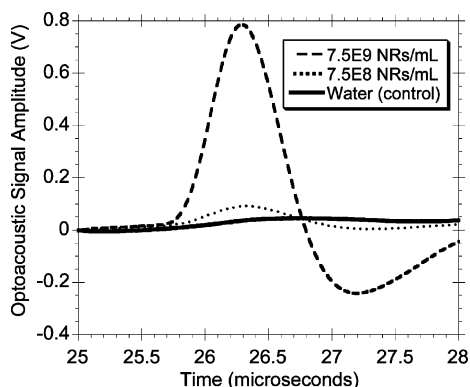


**Figure 2.** Optoacoustic signal generated by Au-NRs detected through a 4 cm thick scattering media. The *x*-axis represents the time following triggering of laser pulse. Au-NRs were detectable at a concentration of  $7.5 \times 10^8$  NRs per mL (1.25 pM).

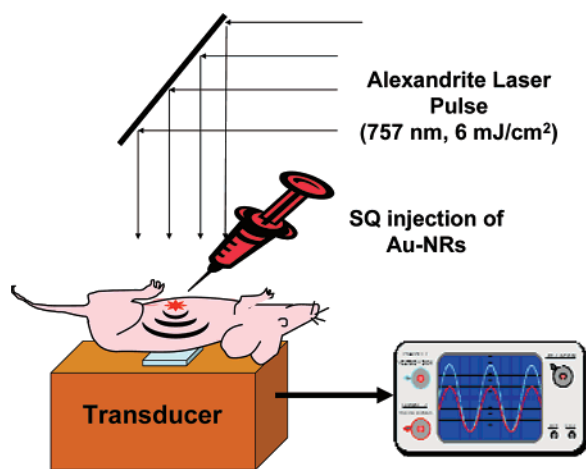


**Figure 3.** Schematics of in vivo experiment to detect subcutaneously (SQ) injected gold nanorods (Au-NRs) using a single-channel acoustic transducer. Au-NRs were injected subcutaneously to lower abdomen and optoacoustic signal was detected from back. The animal was sedated to minimize motion artifact.

Au-NRs that targeted tumors located deep within tissue. An in vivo experiment was conducted to determine if optoacoustic method could be used for single-point detection of subcutaneously injected Au-NRs in nude mice. Figure 3 shows the schematics of this experiment in which optoacoustic detection was performed in the forward mode. A nude mouse (Hsd:ATHymic Nude-Foxn1nu, Harlan Bioproducts for Science, Indianapolis, Indiana) was anesthetized by intraperitoneal injection of a mixture of xylazine/ketamine and was placed in a supine position (face up) on top of a single-channel optoacoustic transducer that was used in the in vitro studies. The same laser source was used to illuminate the abdomen of the mouse at a fluence of  $6 \text{ mJ/cm}^2$ .

Initially, optoacoustic signals were recorded before and after subcutaneous injection of  $25 \mu\text{L}$  of PBS as control. The results indicated that the injection of PBS did not change the profile of optoacoustic signal. Then, stock solution of PSS-coated Au-NRs at concentrations of 125, 12.5, and 1.25 pM was prepared by centrifugation and serial dilution in PBS. Then  $25 \mu\text{L}$  of each solution was injected subcutaneously at several sites within the lower abdominal region of the mouse.

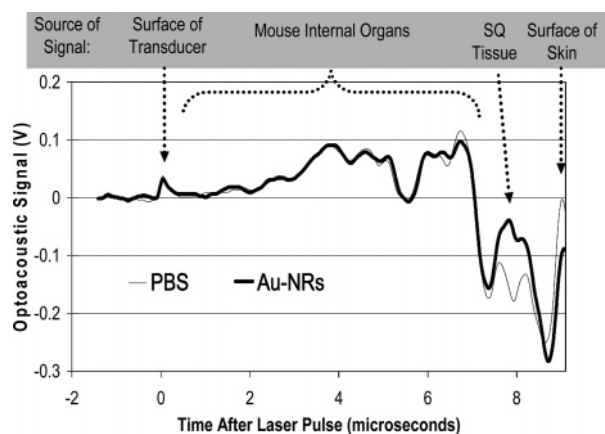


**Figure 4.** In vivo detection of injected gold nanorods (Au-NRs) in nude mouse using a single optoacoustic transducer. Suspension of gold nanorods ( $25 \mu\text{L}$  at a concentration of 1.25 pM) or PBS ( $25 \mu\text{L}$ ) was injected subcutaneously (SQ) into the abdominal area of mouse to enhance optoacoustic signal where the signal was detected via a transducer placed on the back of the mouse. The *x*-axis represents the time of arrival of signal in microseconds with zero representing the time of arrival of signal generated at the surface of transducer. The time of arrival of the signal originated from injected Au-NRs was  $8 \mu\text{s}$ , which corresponds to a distance of 12 mm from the surface of transducer. As compared to PBS injection, subcutaneously injected Au-NRs increased the amplitude of optoacoustic signal by enhancing local light absorption. A graph depicting the difference between PBS and Au-NRs traces is available as Supporting Information.

An optoacoustic signal from each site corresponding to various concentrations of gold particles was recorded. This procedure was repeated several times to measure the minimum detectable concentration of injected Au-NRs. The results were consistent and reproducible. Figure 4 is a typical optoacoustic signal that was recorded in these series of experiments.

In Figure 4, the *x*-axis is the time of arrival of the signal in microseconds with zero being the time of arrival of signal from the surface of transducer. Note that, in this scale, laser pulse was delivered at  $-2.5 \mu\text{s}$ . The first peak represents the generation of acoustic waves as the laser light interacts with the surface of transducer. By assigning zero to this time point, one would be able to determine the distance of other objects from the surface of transducer by multiplying the time of arrival of signal by the speed of sound in tissue ( $\sim 1.5 \text{ mm}/\mu\text{s}$ ). For instance, the thickness of the lower mouse abdomen in this experiment was measured as  $\sim 13 \text{ mm}$ . In other words, the skin over the mouse abdomen was 13 mm away from the surface of transducer that was placed in the back of animal. Because of this, the signal generated in the skin of the mouse reached the transducer after approximately  $9 \mu\text{s}$  ( $9 \mu\text{s} \times 1.5 \text{ mm}/\mu\text{s} = 13.5 \text{ mm}$ ). Au-NRs were injected  $\sim 1 \text{ mm}$  underneath the skin (SQ); thus, their optoacoustic signal was expected to arrive less than  $1 \mu\text{s}$  earlier than that of skin. Figure 4 shows that the optoacoustic profile following PBS and Au-NRs injection were almost identical except for the area around  $8 \mu\text{s}$ , where injected Au-NRs increased the amplitude of optoacoustic signal by enhancing local light absorption in subcutaneous area (SQ). As expected, the amplitude of optoacoustic signal at this time point

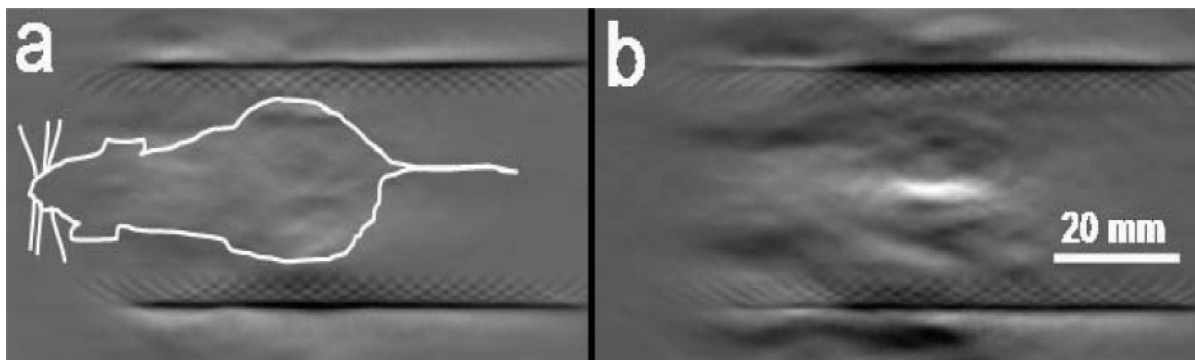


**Figure 5.** A typical optoacoustic image of a nude mouse before (a) and after (b) subcutaneous injection of 100  $\mu\text{L}$  of Au-NRs at a concentration of  $7.5 \times 10^{10}$  NRs per mL in the abdominal area. Injected nanoparticles were brightly visible in the optoacoustic image (b). Drawing in (a) depicts the approximate position of the nude mouse during experiment.

increased proportionally when higher concentrations of Au-NRs were injected (data not shown). This experiment shows that the optoacoustic method can be used for the single-point detection of Au-NRs when a minimum of 25  $\mu\text{L}$  of Au-NRs at a concentration of 1.25 pM was injected subcutaneously. Note that by using several acoustic transducers and applying time-resolved algorithms, one would be able to locate the exact location of Au-NRs within the tissue.

To further demonstrate the capability of LOIS to generate an image of the distribution of Au-NRs in vivo, another experiment was designed to image a nude mouse before and after subcutaneous injection of Au-NRs. To perform this experiment, a custom optoacoustic imaging system was designed and assembled at Fairway Medical Technologies, Houston, TX. The transducer that was used in this experiment was composed of two parallel linear arrays of 32 acoustic transducers equipped with a real-time multichannel signal processor that provided a gain of over 30 dB and a noise level less than 2 mV for acoustic detection. A nude mouse was anesthetized as described before, was placed between two linear probes (transducer arrays), and the laser irradiation was delivered orthogonally to the image plane. To perform this experiment, we had to expand the laser beam more to illuminate the whole body of mouse. Because of additional expansion of the laser beam, the fluence dropped to 2 mJ/cm<sup>2</sup>, as compared to previous experiments where the fluence was 6 mJ/cm<sup>2</sup>. Lower fluence resulted in a diminished optoacoustic signal. Also, the gain of multichannel transducer array used in this experiment was less than that of the previously used single-channel transducer due to its size and its electronic design (gain of 30 dB vs 60 dB). To minimize the effects of these limitations, more Au-NRs had to be injected in this experiment as compared to what was used for single-point measurements. After acquiring a control image, 100  $\mu\text{L}$  of a solution of PEGylated Au-NRs at a concentration of  $7.5 \times 10^{10}$  NRs per mL was injected subcutaneously into the abdominal area of a nude mouse and optoacoustic images were acquired. Figure 5 depicts the result of this experiment.

Figure 5a shows the optoacoustic imaging of the nude mouse before injection of Au-NRs. The body of the mouse was hardly visible in the optoacoustic image due to the low ultrasound frequency cutoff in our imaging system, and thus

an overlay drawing is added to Figure 5a to illustrate the approximate position of the animal during this experiment. Figure 5b, which was captured after subcutaneous injection of Au-NRs, shows the enhancement of optoacoustic signal in the area that Au-NRs were injected. The injected Au-NRs were brightly visible in the optoacoustic image while the body of the mouse was almost invisible. This is due to the presence of the high contrast between normal tissue and Au-NRs under optoacoustic imaging. This experiment successfully demonstrated the feasibility of using LOIS to image gold nanorods in vivo.

The National Cancer Institute has recognized nanotechnology as an extraordinary opportunity to detect and/or treat cancer.<sup>20</sup> Gold nanoparticles are attractive because they appear to be biocompatible<sup>17,18,21,22</sup> and can be produced with the desired physical and chemical properties. Gold nanoparticles can be made in various shapes and dimensions,<sup>23</sup> among which Au-NRs are especially interesting as contrast agents for optoacoustic imaging because they provide the strongest absorption relative to their size.<sup>24</sup> Gold nanoparticles can be functionalized by conjugating them to other molecules such as tumor ligands, DNA, or monoclonal antibodies to perform a biological task.<sup>20</sup>

It would be useful to compare the sensitivity of the optoacoustic method for the detection of Au-NRs to the sensitivity of alternate methods such as MRI for the detection of ferrimagnetic nanoparticles. According to the data presented in Figure 2, the minimum concentration of Au-NRs with an average dimension of 50 nm  $\times$  15 nm that is detectable within gelatin phantoms using the optoacoustic method is less than  $7.5 \times 10^8$  NRs/mL (1.25 pM); this concentration of Au-NRs corresponds to 0.13  $\mu\text{g}$  Au per mL (i.e., multiply the total volume of particles in each mL of solution by the specific weight of gold, 19.3 g/mL). In comparison, Pardoe et al. used similar gelatin phantoms in their experiment and reported that the minimum concentration of ferrimagnetic nanoparticles that is detectable using MRI is 10  $\mu\text{g}$  Fe per mL.<sup>25</sup> This means that the sensitivity of optoacoustic method to detect Au-NRs in vitro is 75 times better than that of MRI to detect ferrimagnetic nanoparticles. MRI is supposed to maintain its sensitivity in vivo; however, the in vivo sensitivity of the optoacoustic method to detect Au-NRs would be affected by the light absorption of

surrounding tissue. Data presented in Figure 4 shows that, at least for mouse skin, which has a modest light absorption in NIR, 25  $\mu\text{L}$  of Au-NRs at a concentration of 1.25 pM ( $\sim 0.13 \mu\text{g Au per mL}$ ) yields detectable optoacoustic signal.

In this work, we have demonstrated that: (1) Au-NRs can be engineered with the desired optical properties that are optimized for in vivo imaging; this includes engineering Au-NRs that absorb strongly at the NIR region of the spectrum where the light absorption of background tissues is minimal to allow deep imaging. (2) Au-NRs can be modified chemically to enhance their biocompatibility and stability; this is particularly important for in vivo applications. (3) The laser optoacoustic method can be used to detect and localize Au-NRs at a very low concentration deep within tissue where other methods such as diffuse optical tomography fail to detect their targets.<sup>25</sup> The high sensitivity of the optoacoustic method is due to the high contrast between light absorption of normal tissues and Au-NRs in the NIR.

The ability to detect Au-NRs at a very low concentration deep within a tissue using optoacoustic methods, along with the fact that Au-NRs can be attached to vehicles such as monoclonal antibodies to target cancer cells,<sup>26</sup> is promising in the development of new diagnostic modalities that employ optoacoustic methods targeting Au-NRs as molecular-specific contrast agents for the early detection of cancer.

**Acknowledgment.** We thank Fairway Medical Technologies and Seno Medical Instruments for their valuable collaboration. This project was supported by NIH (grant no. R44CA110137), Breast Cancer Imaging Research Program from the U.S. Army (grant no. W81XWH-04-1-0484), and NSF (grant no. 427590).

**Supporting Information Available:** The difference between control and Au-NRs signal traces presented in Figure 4. This material is available free of charge via the Internet at <http://pubs.acs.org>.

## References

- (1) Yezhelyev, M. V.; Gao, X.; Xing, Y.; Al Hajj, A.; Nie, S.; O'Regan, R. M. *Lancet Oncology* **2006**, *7*, 657–667.
- (2) Ferrari, M. *Nat. Rev. Cancer* **2005**, *5*, 161–171.
- (3) Gao, X.; Cui, Y.; Levenson, R. M.; Chung, L. W. K.; Nie, S. *Nat. Biotechnol.* **2004**, *22*, 969–976.
- (4) Oraevsky, A.; Karabutov, A. Optoacoustic Tomography. In *Biomedical Photonics Handbook*, 2003 ed.; Vo-Dinh, T., Ed.; CRC Press: Boca Raton, FL, 2003; Chapter 34, pp 34-1–34-34.
- (5) Wilson, B. C. Appendix to Chapter 8: Summary of Optical Properties. In *Optical-Thermal Response of Laser-Irradiated Tissue*, Welch, A. J., Van Gemert, M. J. C., Eds.; Plenum: New York, 1995; Chapter 8, pp 275–303.
- (6) Kruger, R. A.; Liu, P. Y.; Fang, Y. R.; Appledorn, C. R. *Med. Phys.* **1995**, *22*, 1605–1609.
- (7) Oraevsky, A. A.; Oraevsky, A. N. *Quantum Electron.* **2002**, *32*, 79–82.
- (8) Hu, M.; Chen, J. Y.; Li, Z. Y.; Au, L.; Hartland, G. V.; Li, X. D.; Marquez, M.; Xia, Y. N. *Chem. Soc. Rev.* **2006**, *35*, 1084–1094.
- (9) Copland, J. A.; Eghtedari, M.; Popov, V. L.; Kotov, N.; Mamedova, N.; Motamedi, M.; Oraevsky, A. A. *Mol. Imaging Biol.* **2004**, *6*, 341–349.
- (10) Cerussi, A. E.; Berger, A. J.; Bevilacqua, F.; Shah, N.; Jakubowski, D.; Butler, J.; Holcombe, R. F.; Tromberg, B. J. *Acad. Radiol.* **2001**, *8*, 211–218.
- (11) Wang, Y. W.; Xie, X. Y.; Wang, X. D.; Ku, G.; Gill, K. L.; O'Neal, D. P.; Stoica, G.; Wang, L. V. *Nano Lett.* **2004**, *4*, 1689–1692.
- (12) Eghtedari, M.; Copland, J. A.; Popov, V. L.; Motamedi, M.; Kotov, N.; Oraevsky, A. A. Bioconjugated Gold Nanoparticles as a Contrast Agent for Optoacoustic Detection of Small Tumors. In *Proc. SPIE*; SPIE: Bellingham, WA, 2003; pp 76–85.
- (13) Guzatov, D. V.; Oraevsky, A. A.; Oraevsky, A. N. *Quantum Electron.* **2003**, *33*, 817–822.
- (14) Dreher, M. R.; Liu, W. G.; Michelich, C. R.; Dewhurst, M. W.; Yuan, F.; Chilkoti, A. *J. Natl. Cancer Inst.* **2006**, *98*, 335–344.
- (15) Lee, K. S.; El Sayed, M. A. *J. Phys. Chem. B* **2006**, *110*, 19220–19225.
- (16) Sau, T. K.; Murphy, C. J. *Langmuir* **2004**, *20*, 6414–6420.
- (17) Connor, E. E.; Mwamuka, J.; Gole, A.; Murphy, C. J.; Wyatt, M. D. *Small* **2005**, *1*, 325–327.
- (18) Niidome, T.; Yamagata, M.; Okamoto, Y.; Akiyama, Y.; Takahashi, H.; Kawano, T.; Katayama, Y.; Niidome, Y. *J. Controlled Release* **2006**, *114*, 343–347.
- (19) Gole, A.; Murphy, C. J. *Chem. Mater.* **2005**, *17*, 1325–1330.
- (20) Cuenca, A. G.; Jiang, H. B.; Hochwald, S. N.; Delano, M.; Cance, W. G.; Grobmyer, S. R. *Cancer* **2006**, *107*, 459–466.
- (21) Ditrich, H.; Splechtna, H. *Tissue Cell* **1988**, *20*, 891–898.
- (22) Hainfeld, J. F.; Slatkin, D. N.; Focella, T. M.; Smilowitz, H. M. *Br. J. Radiol.* **2006**, *79*, 248–253.
- (23) Malikova, N.; Pastoriza-Santos, I.; Schierhorn, M.; Kotov, N. A.; Liz-Marzan, L. M. *Langmuir* **2002**, *18*, 3694–3697.
- (24) Jain, P. K.; Lee, K. S.; El Sayed, I. H.; El Sayed, M. A. *J. Phys. Chem. B* **2006**, *110*, 7238–7248.
- (25) Pardoe, H.; Chua-anusorn, W.; St Pierre, T. G.; Dobson, J. *Phys. Med. Biol.* **2003**, *48*, N89–N95.
- (26) Bernard-Marty, C.; Lebrun, F.; Awada, A.; Piccart, M. J. *Drugs* **2006**, *66*, 1577–1591.

NL070557D